FRACTURE ANALYSIS OF FILAMENT-WOUND FRP COMPOSITES USING RING BURST TEST

Shuichi Wakayama, Akihiro Horide and Masanori Kawahara

Department of Mechanical Engineering, Tokyo Metropolitan University,
1-1 Minami-Ohsawa, Hachioji-shi, Tokyo 192-0397, Japan

SUMMARY: New testing technique, ring burst test, was developed for the investigation of the fracture behavior of filament winding (FW)-FRP composites. The internal pressure can be applied to the ring shaped specimens similarly to the burst tests of actual pressure vessels. The uniform deformation in specimen was confirmed by strain measurement and FEM analysis. It is important that the fracture behavior inside of the FRP layers could be observed directly while it is impossible to observe the fracture behavior under the surface of actual pressure vessels. In order to demonstrate the advantages of ring burst test, the fracture analysis of FW-FRP, with the various degree of fiber waviness, was carried out using in situ observation and AE measurement. Consequently, the effect of fiber waviness on the strength of FW-FRP was understood by using ring burst test.

KEYWORDS: filament wound FRP composite, ring burst test, FEM analysis, strain distribution, NOL ring tensile test, acoustic emission analysis, fiber waviness

INTRODUCTION

FW-FRP pressure vessels have been developed and applied in industries due to the high specific strength. However, it is frequently reported that the strength of the FW-FRP components is lower than expected value, which is caused by the influence of inhomogeneous microstructures such as fiber waviness on the fracture process [1–3]. Then, the fracture analysis using various testing techniques has been carried out. For an example, the NOL ring tensile test is one of the simplified method for the fracture investigation in FW-FRP components but it is well known that the deformation is concentrated at the edge of semi-circular loading apparatus.

For the above reasons, the ring burst test was developed by the authors [4-6]. The internal pressure, which is equivalent to the actual pressure vessels, can be applied to ring shaped FW-FRP specimens during the ring burst tests. Furthermore, the fracture behavior inside of FRP layers can be observed directly. In order to demonstrate the advantages of ring burst test, the fracture analysis of the FW-FRP composites containing fiber waviness was carried out. It was reported that the formation of waviness was caused by thermal shrinkage during curing and the compressive deformation of inner layer by the binding of outer layer (bandage effect) during filament winding [3]. Then, in this study, the tension in fiber was controlled during filament winding to obtain the various degree of fiber waviness.

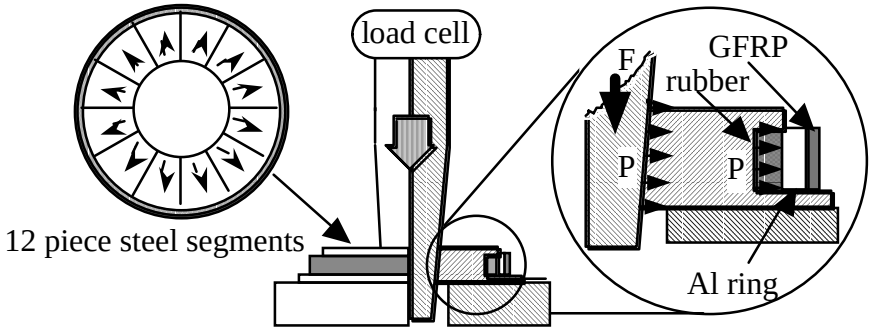

In this paper, the ring burst tests were applied to the evaluation of the strength and the investigation of the fracture behavior in FW-FRP composites. Strain distribution in specimen was measured and analyzed by FEM calculation. Fracture process during the tests was investigated by in situ observation and AE analysis. The purposes of this paper are to understand the effect of fiber waviness on strength and to demonstrate the advantages of the ring burst test for the fracture analysis of FW-FRP structures.

EXPERIMENTAL PROCEDURE

Ring Burst Test

A schematic drawing of the ring burst test equipment is shown in Fig. 1. The internal pressure was generated by means of inserting a tapered rod into twelve piece steel segments. The specimen was then pressurized through an urethane rubber ring located between the specimen and the twelve piece segments. Since the internal pressure applied to the specimen could not be measured directly during the ring burst test, the preparatory experiments were carried out using the high strength steel ring as a calibration specimen.

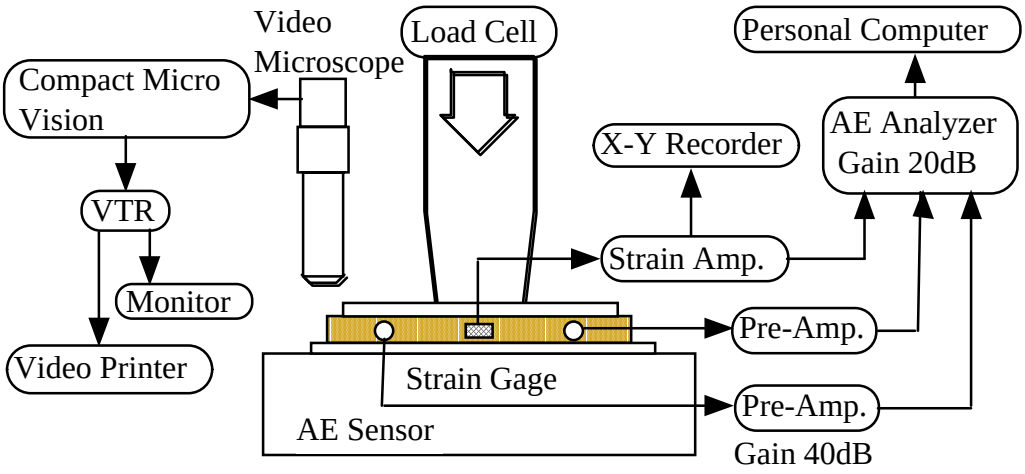

Figure 2 shows the diagram of measuring system. Ring burst tests are carried out using a computer-controlled hydraulic testing machine in air under constant rod speed. Strain in outermost FRP ply was measured by strain gages on the surface. The deformation and fracture process in FRP layers was observed by high magnification video system as shown in the figure. In order to obtain the information on microfracture process such as fiber breakage and interlaminar friction, AE measurement was also carried out using 2 ch sensors attached on the specimen. The AE signals as well as axial load and strain data were measured by AE system, simultaneously.

Preparation of the Specimen

FRP ring specimens were made from the E-glass fiber (roving tensile strength: 1.9 GPa) and the epoxy resin. The fiber roving with the epoxy resin was wound along the hoop direction at the pitch of 5 mm on the aluminum tube (A6061-O, outer diameter: 100 mm, thickness: 3 mm) by the filament winding machine. After curing at 150 ^{o}C for 4 hours in an oven, the FRP wound on aluminum tubes were cut to the ring specimens of 10 mm in width.

In order to obtain the various specimens with different degree of fiber waviness, the tension in fiber was controlled during filament winding. The fiber tension was tabulated in Table 1. The tension was increased from 16 N to 19 N (Type I) or decreased from 16 N to 8.5 N (Type D) gradually, or kept constant at 16 N (Type C).

Table 1: Winding tension in fiber roving during filament winding

Ply Number		1 st	2 nd	3 rd	4 th	5 th	6 th	7 th
Average Tension [N]	Type C Constant Tension	15.9	16.3	15.7	15.1	15.2	15.0	15.3
	Type I Increasing Tension	16.0	16.8	17.4	18.1	18.4	18.9	19.2
	Type D Decreasing Tension	16.3	15.2	14.0	12.6	11.5	10.6	8.56

EXPERIMENTAL RESULTS

Deformation Behavior of Specimens during Ring Burst Tests

In order to obtain the relationship between axial load in tapered rod and corresponding internal pressure, the high strength steel ring with same size as aluminum tube was used for calibration specimen. Figure 3 shows the relationship between circumferential and axial strain in steel ring and axial load in tapered rod. It can be seen in the figure that circumferential strain increased linearly with increasing load. On the other hand, axial strain was compressive according to Poisson's ratio of steel. The circumferential stress can be calculated from circumferential strain using Hooke's law and then supposing the steel ring as thin wall cylinder, corresponding internal pressure can be obtained. Finally, the linear relationship between the corresponding internal pressure, P, and the axial load of rod, F, was obtained as following equation.

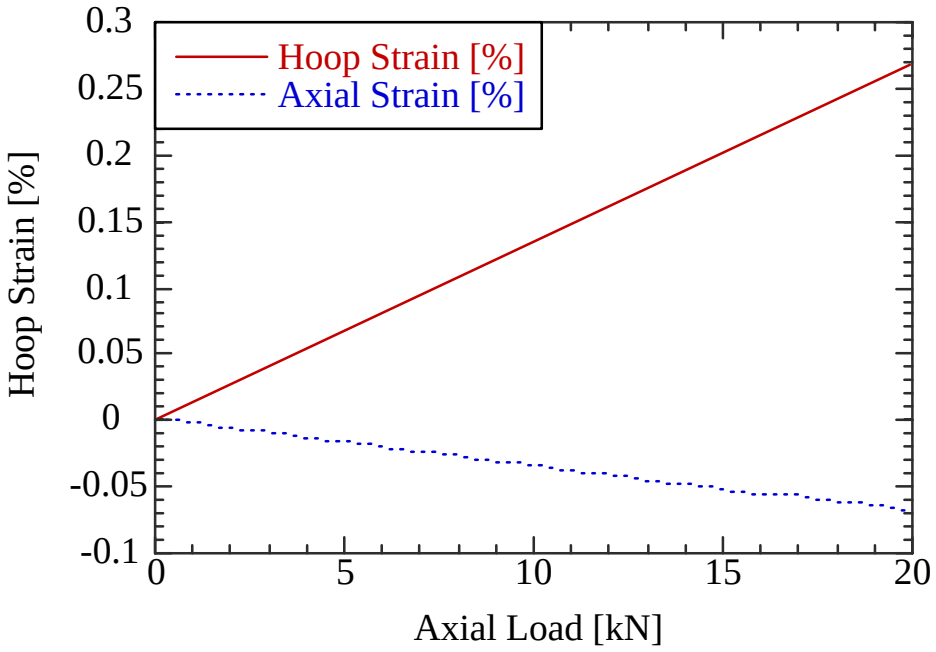
Hoop Strain [%]
Axial Strain [%]
Hoop Strain [%]
Axial Load [kN]
0.3
0.25
0.2
0.15
0.1
0.05
0
-0.05
-0.1
0
5
10
15
20

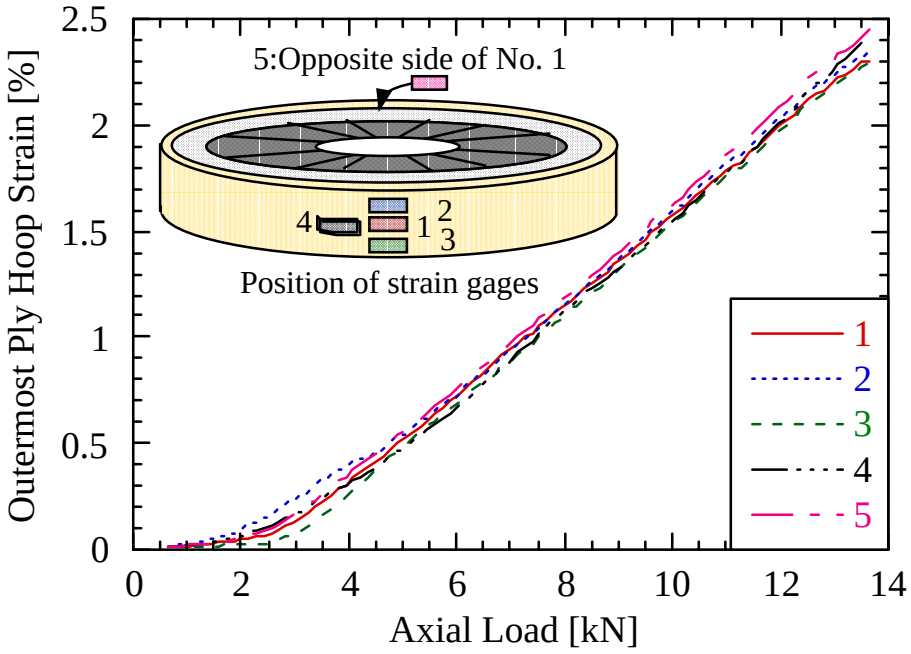
5:Opposite side of No. 1
4
1
2
3
Position of strain gages
1
2
3
4
5
Outermost Ply Hoop Strain [%]
Axial Load [kN]
2.5
2
1.5
1
0.5
0
0
2
4
6
8
10
12
14

$$P\ [MPa]=1.772\ F\ [kN] \quad (1)$$

It is important that this relationship shows good reproductiveness.

The relationship between hoop strain and axial load obtained during the ring burst test of FW-FRP composite ring is shown in Fig. 4. The hoop strain was measured at each gage positions indicated in the figure. It is understood from the strain behaviors of No.1 and 4 that the deformation at the edge and center of loading segment is uniform. The uniform deformation along the longitudinal axis is also described by the agreement among strain behaviors of No.1, 2 and 3.

Burst Strength of FW-FRP Composite Ring

The results of ring burst tests are tabulated in Table 2. Numbers of specimens are 3 to 5 for each type and ply number specimens. Volume fraction of fiber of all specimens is almost 50 %. It is understood from the table that the burst strain of outermost ply is almost 2.5 %, which is equivalent to the failure strain of fiber roving independently from the specimen type or ply number. Since the ring burst tests were carried out under constant rod speed, it was observed that the inner plies remained after the failure of outer plies. Therefore, it is strongly suggested that strain in inner plies were lower than that in outermost ply at the failure.

On the other hand, the burst pressure, obtained from the axial load at the failure using Eqn (1), increases with increase in number of plies. It is significant that, comparing the strength of same ply number specimens with different type, the strength of Type I (increasing fiber tension) is lower than that of Type C (constant fiber tension) and that of Type D (decreasing fiber tension) is higher than that of Type C. Especially, 7 ply Type D specimen has the strength 10 % higher than 7 ply Type I specimen. Consequently, it can be concluded that the burst pressure of FW-FRP composite is successfully enhanced by controlling the tension in fiber during filament winding.

Table 2:Results of ring burst tests of FW-FRP composites

Tension condition (Specimen type)	Constant (C)				Increasing (I)				Decreasing (D)			
Number of plies	2	3	5	7	2	3	5	7	2	3	5	7
Number of specimens	3	4	3	3	3	3	5	4	3	4	5	3
V_f [%]	52	52	56	56	46	48	51	56	52	53	50	54
Thickness of FRP [mm]	0.71	1.07	1.78	2.31	0.79	1.18	1.84	2.34	0.81	1.12	1.84	2.39
Average burst strain [%]	2.56	2.19	2.12	2.26	2.24	2.44	2.30	2.23	2.59	2.29	2.47	2.35
Average burst pressure [MPa]	19.1	24.9	37.1	50.9	18.9	24.8	37.5	48.8	19.5	25.0	38.7	53.7

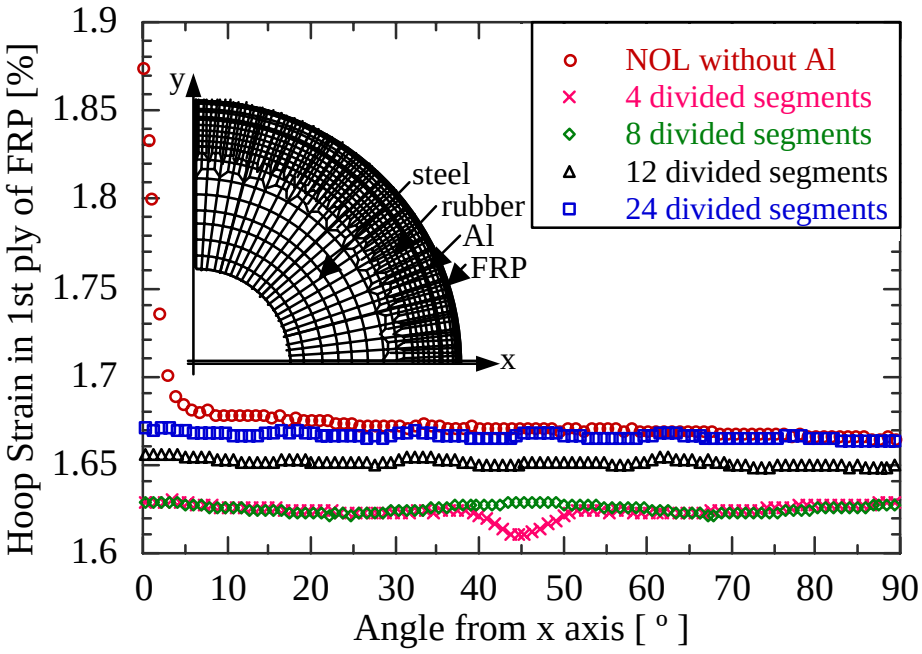

DISCUSSION

Strain Distribution of Ring Specimen during Ring Burst Test

The distribution of hoop strain in the outermost ply of the FRP ring specimen was uniform as shown in Fig. 4. In order to investigate the effect of number of segments on the strain distribution, the deformation process during ring burst test was analyzed by 2 dimensional FEM calculation. 8 node isoparametric quadrilateral plain strain elements are used in the FEM code (MARC). Considering the symmetry, one quarter of 2 ply FRP specimen with ring burst test apparatus was modeled and the total number of elements was 1416.

Figure 5 shows the distribution of hoop strain in 1st ply FRP. Used FEM model was also indicated in the figure. For the comparison, NOL ring tests, which corresponds to the case of 2 segments except for Al ring, was also analyzed. The edges of segments locate at 0^o for NOL, 45^o for 4 segments, 22.5^o and 67.5^o for 8 segments, 15^o, 45^o and 75^o for 12 segments, and 7.5^o, 22.5^o, 37.5^o, 52.5^o, 67.5^o and 82.5^o for 24 segments, respectively. In the figure, quite large strain concentration is observed at the edge of NOL ring test. On the other hand, it is understood that the strain distribution becomes uniform as the number of segments increases.

The ratio of variation to average of hoop strain in 1st FRP layer is tabulated in Table 3. The variation ratio for the segments more than 8 is smaller than 0.5 %, then it can be concluded that number of segments used in the present study, 12, is large enough.

Table 3: Effect of number of segments on strain variation ratio

Division number of segments	NOL ring	4	8	12	24
Strain variation ratio [%]	12.5	1.20	0.480	0.497	0.444

Fracture Process of FW-FRP Composite Ring during Ring Burst Tests

The burst strength of the FW-FRP ring specimens was evaluated using the ring burst tests. During the tests, the in situ observation of the deformation behavior in FRP layers was carried out. It was then observed that the waviness in each layer was cancelled in order from outer to inner layer. It is important that these behavior was observed most frequently in Type I (increasing tension) specimens. In some cases, the waviness cancellation might occur out of the observation area. Therefore, the cancellation was also detected by AE measurement using AE parameter analysis [5, 6]. Finally, the hoop strain in outermost ply at the waviness cancellation of inner plies was determined from in situ observation and AE analysis.

As shown in Table 2, Type D (decreasing tension) specimen has the largest strength in same ply number specimens with 3 type tension conditions, especially in the specimens with large number of plies. Considering these characteristics of strength and waviness cancellation behavior, it is concluded that the burst pressure of FW-FRP composites can be enhanced due to the restraint of fiber waviness by controlling the tension in fiber during filament winding. In order to understand the mechanism of the effect of fiber waviness on burst strength, the burst pressure was predicted according to 2 models, i.e. the ideal model under uniform deformation and the experimental model considering fiber waviness, as followings.

Ideal model

The ideal model is based on the law of mixture, where the hoop strain in all ply is uniform until the final failure of the specimen. Supposing the each FRP ply as thin wall cylinder, the burst pressure of each ply, P_{FRP}, is

$$P_{FRP} = \sigma_{FRP} \frac{t_{FRP}}{r_{FRP}} \tag{2}$$

where t_{FRP}, r_{FRP} and σ_{FRP} are the thickness, radius and strength of FRP ply, respectively. Supposing the burst strain of all plies is failure strain of fiber roving (2.5 %), σ_{FRP} is obtained from the Young's modulus and becomes constant for all FRP plies.

Radius and thickness of FRP plies can be considered as constant. The ideal burst pressure, P_{ideal}, is then simply derived from the superposition of the burst pressure of each ply as following equation.

$$P_{ideal} = P_{Al} + N\, P_{FRP} \tag{3}$$

where P_{Al} is burst pressure of Al ring and N is the number of FRP plies.

Experimental model

In the experimental model, the deformation behaviors of each FRP plies of 5 ply specimen are considered as described in Fig. 6. Before the cancellation of waviness, hoop stress and strain in every ply is uniform. When the strain becomes some specific value, the cancellation of all

of waviness in the ply occurs simultaneously. Then the stress and strain in the ply decrease corresponding to the length of waviness. The decrease in stress remains until the failure of outermost ply.

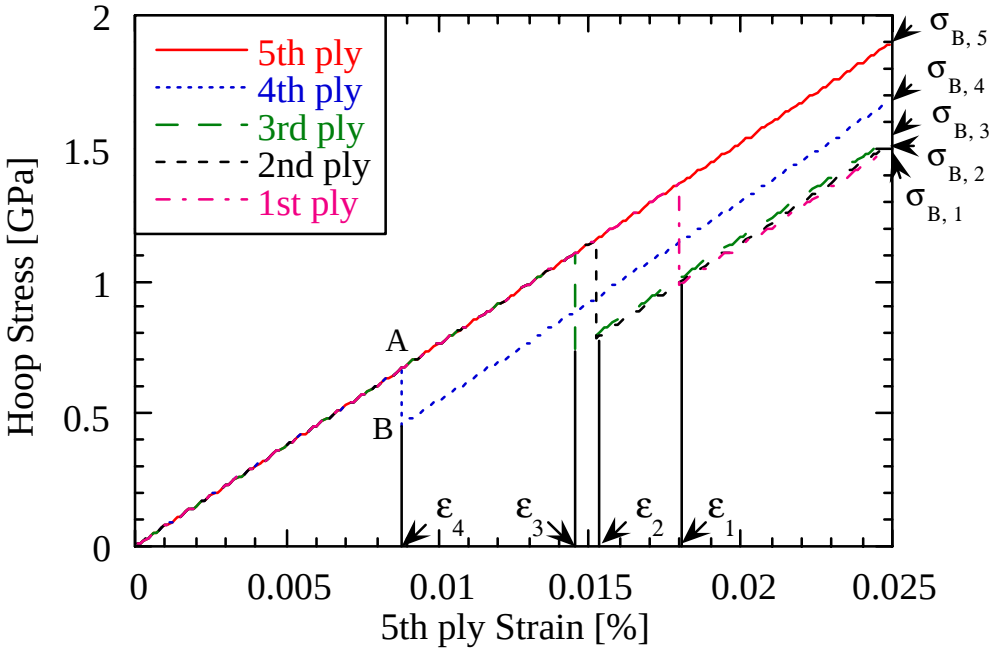

In this model, it is essential to estimate the length of waviness. However, it is quite difficult to determine the waviness length theoretically or experimentally, because the mechanism of the waviness formation has not been understood well. Therefore, it is assumed in this paper that the length of waviness is the twice of the difference in radius of the ply before and after the cancellation of waviness.

According to these assumptions, the decrease in strain due to the cancellation of fiber waviness of i-th (i = 1, 2, … , N) ply of N ply specimen can be derived as

$$\varepsilon_i - \varepsilon_i' = \frac{\varepsilon_i(\varepsilon_i + 1)}{\pi + \varepsilon_i} \tag{4}$$

where ε_i and ε_i' are the hoop strain in i-th ply before and after the cancellation of the fiber waviness. Because the outermost (N-th) ply does not contain the waviness, ε_i is equal to 0, then Eqn (4) becomes 0.

Supposing that Young's modulus is constant before and after the cancellation, the hoop stress of i-th ply at the failure of outermost ply can be calculated using Young's modulus of FRP. Finally, the burst pressure of N ply specimen, P_{exp}, containing the fiber waviness can be obtained by the superposition of the burst pressure of each plies.

$$P_{\exp} = P_{Al} + \sum_{i=1}^{N} P_{FRP,i} = P_{Al} + \sum_{i=1}^{N} \sigma_{B,i} \frac{t_{FRP}}{r_{FRP}} \tag{5}$$

where $P_{FRP,i}$ and $\sigma_{B,i}$ are the internal pressure and hoop stress in i-th ply at the failure of N-th ply, respectively. When the fiber waviness is not contained in the specimen, $\sigma_{B,i}$ is equal to $\sigma_{B,N}$, then Eqn (5) becomes equivalent to Eqn (3).

Table 4: Comparison of calculated strength and experimental result

Number of ply	2		3		5		7	
Specimen type	Type I	Type D	Type I	Type D	Type I	Type D	Type I	Type D
Experimental result [MPa]	18.9	19.5	24.8	25.0	37.5	38.7	48.8	53.7
Ideal model [MPa] (Exp. / model)	19.9 (0.95)	19.9 (0.98)	27.2 (0.91)	27.2 (0.92)	41.6 (0.90)	41.6 (0.93)	55.9 (0.87)	55.9 (0.96)
Experimental model [MPa] (Exp. / model)	18.3 (1.03)	18.4 (1.06)	24.1 (1.03)	25.0 (1.00)	37.3 (1.01)	37.6 (1.03)	49.7 (0.98)	52.5 (1.02)

Effect of fiber waviness on burst pressure

The predicted burst pressure by 2 models were compared with the experimental results, as tabulated in Table 4. Comparing the burst pressure obtained from ideal model and experiments, it is understood that the experimental results are lower than the value predicted by ideal model for all specimens. Especially, 7 ply Type I specimen, which contains the largest degree of fiber waviness, has the burst pressure lower than 90 % of the prediction by ideal model.

On the other hand, the burst pressure predicted by proposed experimental model shows good agreement with experimental results. In this study, the length of fiber waviness was obtained from the hoop strain in outermost ply at the cancellation of fiber waviness, which is experimentally determined by in-situ observation of deformation process and AE analysis, using strong assumption. Although further investigation on the mechanism of the formation of fiber waviness is needed, it can be concluded that the effect of the fiber waviness on the burst pressure of FW-FRP composites was well understood.

CONCLUSIONS

In the present study, the new experimental technique, ring burst test, was developed for the investigation of the fracture process and strength of FW-FRP composites. In order to demonstrate the advantages of the proposed testing method, the FW-FRP ring specimens with different degree of fiber waviness were prepared by means of controlling the tension in fiber during filament winding and the ring burst tests of those specimens were carried out. The fracture process was investigated by AE analysis and in situ observation by high magnification video system. Finally, following conclusions were obtained.

1. Uniform hoop strain distribution in the ring specimen during ring burst tests was obtained. It was confirmed by the strain measurement and FEM analysis. The linear relationship between axial load in rod and corresponding internal pressure was obtained by the calibration tests.

2. The in situ observation of inter- and/or intralaminar fracture behavior of FRP layers can be carried out during ring burst tests. Due to the simplicity and low cost of the testing technique, a number of similar tests can be repeated easily comparing with burst tests of actual pressure vessels.

3. The strength of FW-FRP composites can be enhanced by the restraint of he fiber waviness in FRP layers by gradually decreasing the fiber tension during filament winding. The effect of the fiber waviness on the fracture process and strength was well understood by fracture analysis using in situ observation and AE measurement during ring burst tests.

REFERENCES

1. Piggott, M. R., " Mesostructures and their Mechanics in Fibre Composites", *Advanced Composite Materials*, Vol. 6, No. 1, 1996, pp. 75-81.
2. Lee, J. W. and Harris, C. E., "A Deformation – Formulated Micromechanics Model of the Effective Young's Modulus and Strength of Laminated Composites Containing Local Curvature", *Composite Materials: Testing and Design* (Ninth Volume), *ASTM STP 1059*, Garbo, S. P., Ed., American Society for Testing and Materials, Philadelphia, 1990, pp. 521-563.
3. Etemad, M. R., Pask, E. and Besant, C. B., "Hoop Strength Characterization of High Strength Carbon Fibre Composites", *Composites*, Vol. 23, No. 4, 1992, pp. 253-259.
4. Fujishima, O., Wakayama, S. and Kawahara, M., "AE Characterization of the Fracture Behavior during Ring Burst Test of FW-FRP Pressure Vessel", *Progress in Acoustic Emission VII*, Kishi, T., Ed., The Japan Society for Nondestructive Inspection, Tokyo, 1994, pp. 463-468.
5. Horide, A, Wakayama, S. and Kawahara, M., "Acoustic Emission Characteristic during ring Burst Test of FW-FRP Multi-ply Composite", *Nondestructive Characterization of Materials VIII*, Green, R.T., Jr., Ed., Plenum Press, New York, 1996, pp. 641-646.
6. Horide, A., Wakayama, S. and Kawahara, M., "Evaluation of Strength in FW-FRP Composites using Ring Burst Test (Effects of Winding Tension on Fracture Behavior and Strength)", *Transactions of the Japan Society of Mechanical Engineers (A*), Vol. 65, No.631, 1999, *in printing.*